Typical real-world locations impact the time course of object coding

Daniel Kaiser[1,*], Merle M. Moeskops[1], Radoslaw M. Cichy[1]

[1]*Department of Education and Psychology, Freie Universität Berlin, 14195 Berlin, Germany*

[*]*Correspondence to:*

Dr. Daniel Kaiser

Department of Education and Psychology

Freie Universität Berlin

Habelschwerdter Allee 45

14195 Berlin, Germany

danielkaiser.net@gmail.com

Abstract

Everyday visual environments are spatially structured in that objects often appear at typical locations in space: for example, lamps hang from the ceiling, whereas carpets lie on the floor. As a consequence, objects repeatedly occupy similar visual field locations. The long-term experience with these spatial regularities prompts the hypothesis that the visual system is tuned to such retinotopic object locations. A key prediction is that typically positioned objects should be coded more efficiently. To test this prediction, we recorded electroencephalography (EEG) while participants viewed briefly presented objects appearing in their typical locations (e.g., an airplane in the upper visual field) or in atypical locations (e.g., an airplane in the lower visual field). Multivariate pattern analysis applied to the EEG data revealed that object classification depended on positional regularities: Objects were classified more accurately when positioned typically, rather than atypically, already at 140 ms, suggesting that relatively early stages of object processing are tuned to typical retinotopic locations. Our results confirm the prediction that long-term experience with objects occurring at specific locations leads to enhanced perceptual processing when these objects appear in their typical locations. This may indicate a neural mechanism for efficient natural scene processing, where a large number of typically positioned objects needs to be processed.

1 Introduction

Visual objects are enclosed entities that can in principle be moved around freely. However, in everyday environments object positions are often quite constrained. For instance, consider the predictability in the locations of objects in a living room: The sofa is facing the TV, a table is in between the two, a lamp hangs from the ceiling, whereas carpets lie on the floor. This example illustrates that the object content of natural scenes is organized in repeatedly occurring positional structures (Bar, 2000; Chun, 2002). Many previous studies have investigated how inter-object relationships in these positional structures (e.g., lamps appearing above tables) impact behavioral performance and neural processing (Biederman, Mezzanotte, & Rabinowitz, 1982; Kaiser, Stein, & Peelen, 2014; Oliva & Torralba, 2007; Wolfe, Võ, Evans, & Greene, 2011). However, positional object structures often also imply that individual objects are associated with particular locations in space (e.g., lamps appearing in the upper part of a scene). It has recently been proposed that the visual system is tuned to these regularities (Kaiser & Haselhuhn, 2017; Kravitz, Vinson, & Baker, 2008), which could facilitate neural processing for individual objects appearing in their typical real-world locations.

Such location-specific variations in object coding are suggested by previous results that indicate the co-representation of object identity and location information in visual cortex: (1) cortical responses depend on the position of the object in the visual field (Hemond, Kanwisher, & Op de Beeck, 2007; Hasson, Levy, Behrmann, Hendler, & Malach, 2002), (2) object selective cortex contains information about both an object's identity and its location (Cichy, Chen, & Haynes, 2011; Golomb & Kanwisher, 2011; Hong, Yamins, Majaj, & DiCarlo, 2017; Kravitz, Kriegeskorte, & Baker, 2010; Schwarzlose, Swisher, Dang, & Kanwisher, 2008), and (3) information about object identity and location emerge at

similar time points in visual processing (Isik, Meyers, Leibo, & Poggio, 2014; Carlson, Hogendoorn, Kanai, Mesik, & Turret, 2011).

The link between identity and location information in object processing creates the possibility that the two properties interact. In everyday environments, the visual system is repeatedly faced with positional structures, where individual object positions are highly predictable. Through this repeated exposure, retinotopic object-coding mechanisms could get tuned to typical object locations, forming neural channels that integratively process an object's identity and its location. Such location-specific processing channels would enhance the processing of an object when it appears in its typical locations within a scene – and within the visual field. Evidence for such a processing enhancement has been found in the domain of person perception, where typical configurations impact cortical responses to individual face and body parts (Chan, Kravitz, Truong, Arizpe, & Baker, 2010; de Haas et al., 2016; Henriksson, Mur, & Kriegeskorte, 2015). For example, in face-selective visual cortex, response patterns are better discriminable for typically, as compared to atypically, positioned face parts (de Haas et al., 2016), revealing visual processing channels that are tuned to the spatial regularities in the face.

Here, we test the prediction that the positional regularities contained in natural scenes can similarly facilitate the processing of everyday objects appearing in their typical locations. Participants viewed objects associated with upper and lower visual field locations (e.g., a lamp or a carpet) (Figure 1A) while we recorded electroencephalography (EEG). We used multivariate classification on the EEG data (Contini, Wardle, & Carlson, 2017) to track the time course of object coding with high temporal precision. Analyses revealed that after 140ms visual processing of objects is affected by their typical real-

world locations: Objects appearing in their typical locations (e.g., a lamp in the upper visual field and a carpet in the lower visual field) could be decoded more successfully than objects appearing in atypical locations (e.g., a carpet in the upper visual field and a lamp in the lower visual field). These results suggest that early, rather than late, stages of visual processing are tuned to the positional object structure of real-world scenes.

2 Materials and Methods

2.1 *Participants*

Thirty-four healthy adults (mean age 26.4 years, *SD* = 5.4; 23 female) completed the experiment. The sample size was set a-priori, based on considerations regarding statistical power: A sample size of 34 is needed for detecting a simple effect with a medium effect size of $d = 0.5$ with a probability of more than 80%. All participants had normal or corrected-to-normal vision, provided informed consent and received monetary reimbursement or course credits for their participation. All procedures were approved by the ethical committee of the Department of Education and Psychology of the Freie Universität Berlin and were in accordance with the Declaration of Helsinki.

2.2 *Stimuli*

The stimulus set consisted of greyscale images of six objects associated with typical visual field locations, of which three were associated with upper visual field locations (lamp, airplane, and hat) and three were associated with lower visual field locations (carpet, boat, and shoe). For each object, ten exemplars were used (see Figure 1A for stimulus examples). The images were matched for overall luminance (using the SHINE toolbox; Willenbockel et al., 2010) and displayed on a white background.

To ensure that the six objects could be reliably linked to a specific location, we validated the association of the six objects with a specific part of the visual field in two ways. First, we assessed the typical spatial distribution of each object in natural scenes, assuming that natural scene photographs represent a snapshot of the visual field roughly approximating natural viewing conditions. Hence, the distribution of the objects in the scene image should be similar to their distribution across the visual field. To objectively measure the typical position of each object within a scene, we queried a huge number of

scene photographs (>100,000) from the LabelMe toolbox, where human observers annotated single objects by drawing labelled polygons (Russell, Torralba, Murphy, & Freeman, 2008). For all scenes containing a specific object we computed the mean pixel coordinate of the area labeled as belonging to the object and then averaged these positions across scenes. The resulting "typical" object locations showed that, as expected, the upper visual field objects were associated with locations (*y*: vertical coordinate from bottom (0) to top (1) of the scene) in the upper parts of scenes (lamp: $y = 0.61$, $SD = 0.17$; airplane: $y = 0.52$, $SD = 0.20$; hat: $y = 0.53$, $SD = 0.25$), while lower visual field objects were associated with locations in the lower part of scenes scenes (carpet: $y = 0.17$, $SD = 0.13$; boat: $y = 0.33$, $SD = 0.23$; shoe: $y = 0.31$, $SD = 0.20$). The typical location in scenes differed significantly between objects associated with the upper and lower visual field, $t > 13.3$, $p < .001$, for all pairwise comparisons. Figure 1B shows the distribution of object locations along the vertical axis of the scenes, split into 7 bins.

Second, we sought to demonstrate a correspondence between this automated, scene-based measure and people's explicit associations of the objects with particular locations in space. We thus asked a set of participants (between 60 and 70 participants; including the participants of the current study, after the completion of the EEG experiment) to indicate the typical locations in which they expect to see each of the six objects. In this task, participants were asked to drag the image of a single exemplar of each object to its typical location on a computer screen (imagining that the computer screen represents their field of view in a natural scene). The central part of the screen – where the object initially appeared – was blocked (indicated by a grey circle), so that participants (1) could not place the object in a central location of the screen, and (2) had to move the object before proceeding. As expected, participants more often chose upper

133 screen positions (*y*: vertical coordinate from bottom (0) to top (1) of the screen) for the
134 upper visual field objects (lamp: $y = 0.65$, $SD = 0.19$; airplane: $y = 0.67$, $SD = 0.20$; hat: $y =$
135 0.57, $SD = 0.20$), and lower screen positions for the lower visual field objects (carpet: $y =$
136 0.29, $SD = 0.22$; boat: $y = 0.36$, $SD = 0.18$; shoe: $y = 0.30$, $SD = 0.18$). The vertical locations
137 chosen by the participants differed significantly between objects associated with the
138 upper and lower visual field, $t > 6.04$, $p < .001$, for all pairwise comparisons. Figure 1C
139 shows the distribution of vertical object locations on the screen, split into 7 bins. The
140 scene-based measure and participants' explicit assessment thus provided converging
141 evidence for the association of the objects with specific spatial locations.
142

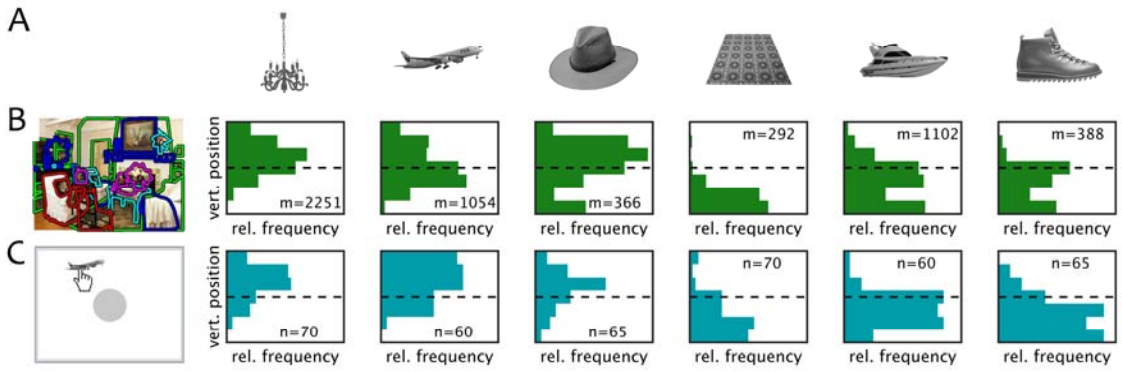

143

144 **Figure 1.** A) Example Stimuli. Ten different exemplar images of six objects each (here, one
145 example image for each object shown) were used as stimuli, of which three objects were
146 associated with the upper visual field (lamp, airplane, hat) and three were associated
147 with the lower visual field (carpet, boat, shoe). B) To validate our assessment of visual
148 field associations, we automatically extracted the positions for each object in a large set
149 of labelled scene photographs taken from the LabelMe scene database (Russell et al.,
150 2008). For each scene, we determined the relative position of the object along the
151 vertical axis, and plotted the distribution across 7 bins (*m:* number of scenes for each
152 object). C) Additionally, we asked a group of participants to indicate for each object the

153 position that it typically occupies in the visual field by dragging the object to the desired
154 location. We then computed the distribution of relative locations along the vertical axis of
155 the screen, split into 7 bins (*n:* number of participants that indicated the typical location
156 for each object). Both measures confirmed the spatial priors associated with the six
157 objects.
158
159 *2.3 Experimental Design*
160 To test whether objects are processed differently when presented in typical and
161 atypical locations within the visual field, the objects were presented in the upper or lower
162 visual field (Figure 2A). On every trial, one object exemplar was presented in one of the
163 two locations for 150ms, followed by a variable inter-trial interval (randomly jittered, from
164 1250ms to 1750ms). Stimuli were presented at 3.25° vertical eccentricity and subtended a
165 visual angle of maximally 3° in horizontal and vertical axes. Stimulus presentation was
166 controlled using the Psychtoolbox (Brainard, 1997). Participants were asked to detect
167 one-back repetitions on an object level (e.g., two different airplanes in direct succession;
168 see Figure 2A). Repetitions occurred on 13% of the trials and equally often for typically and
169 atypically positioned repetition targets and for the top and bottom locations. Participants
170 performed accurately on this task (mean accuracy 96%, *SD* = 2%), with no difference in
171 accuracy between typically and atypically positioned objects, $t(33) = 0.87$, $p = .391$. One-
172 back repetition trials were removed from all EEG analyses. The whole experiment
173 consisted of 1656 trials (including 216 repetition trials). The 1440 non-repetition trials
174 consisted of 12 repetitions of each object exemplar in each location (i.e., 120 repetitions
175 per object and location). The experiment was split into 8 runs, and participants could take
176 breaks between the runs. Twelve participants completed an extended experimental

177 session with 2760 trials (including 360 repetition trials), which additionally contained the
178 same conditions at large eccentricities in half of the trials; these additional data are not
179 reported here. The 2400 non-repetition trials consisted of 10 repetitions of each object
180 exemplar in each of the four locations (i.e., 100 repetitions per object and location). The
181 extended experiment was split into 12 runs.
182

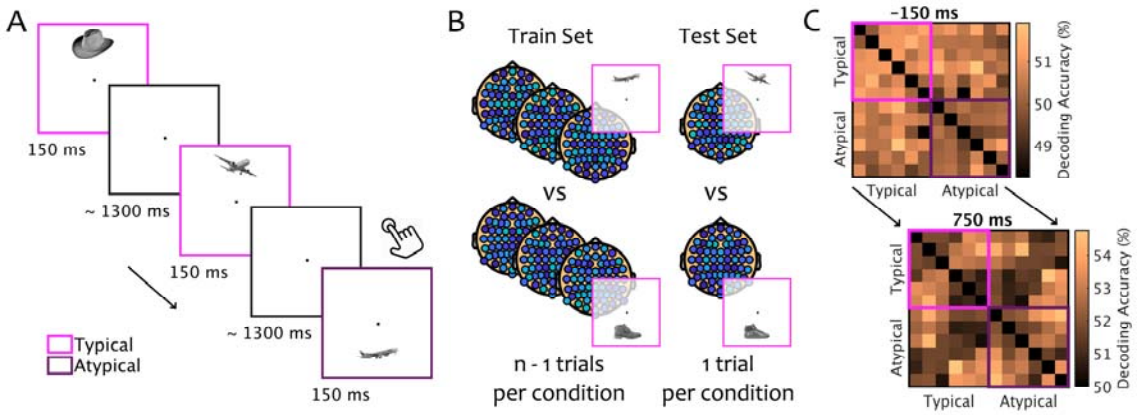

183

184 **Figure 2.** Paradigm and Classification Logic. A) Stimuli were presented for 150 ms in upper
185 or lower visual field locations, corresponding to an object's typical or an atypical location.
186 Participants were instructed to detect occasional one-back repetitions on an object-
187 category level (irrespective of the stimulus location) by pressing a button. Colors
188 indicating the two regularity conditions are shown for illustrative purposes only. B)
189 Multivariate classification was performed on response patterns across all electrodes,
190 separately for each pairwise combination of objects (exemplified here by airplane and
191 shoe in regular locations). The data was split into two sets: a training set consisting of all
192 (but one) trials for each object and a testing set consisting of the two left-out trials. LDA
193 classifiers were repeatedly trained and tested until every trial was left out once and
194 accuracy was averaged across these repetitions. C) The pairwise classification analysis
195 was repeated for each 10 ms time bin, resulting in a 12-by-12 matrix of pairwise

196 classification accuracies (with an empty diagonal) at every time point. To determine
197 differences between typically and atypically positioned objects, pairwise comparisons
198 within the typically placed objects (pink rectangle, upper left) and within the atypically
199 placed objects (purple rectangle, lower right) were averaged and compared (Figure 3).
200
201 *2.4 EEG recording and preprocessing*
202 The EEG was recorded using an EASYCAP 64-channel system and a Brainvision
203 actiCHamp amplifier. The 64 electrodes were arranged in accordance with the standard
204 10-10 system. The data was recorded at a sampling rate of 1000 Hz and filtered online
205 between 0.5 and 70 Hz. For one participant, due to a technical problem, only data from 32
206 electrodes was recorded. All electrodes were referenced online to the Fz electrode.
207 Offline preprocessing was performed in MATLAB, using the FieldTrip toolbox
208 (Oostenveld, Fries, Maris, & Schoffelen, 2011). The continuous EEG data was epoched into
209 trials ranging from 150ms before stimulus onset to 750ms after stimulus onset. Trials
210 containing movement-related artefacts were visually identified and excluded from all
211 analyses. Blink and eye movement artifacts were identified and removed using
212 Independent Components Analysis (ICA) and visual inspection of the resulting
213 components. To increase the signal-to-noise ratio of the classification analyses (Carlson,
214 Tovar, Alink, & Kriegeskorte, 2013), the data was downsampled to 100Hz.
215 *2.5 EEG classification procedure*
216 Multivariate classification analyses were carried out in MATLAB using the
217 CoSMoMVPA toolbox (Oosterhof, Connolly, & Haxby, 2016). Classification was performed
218 separately for each 10ms time bin, resulting in classification time courses with 10 ms
219 resolution. The analysis was performed pairwise, for all possible combinations of the six

objects appearing in the two locations. Linear discriminant analysis (LDA) classifiers were always trained and tested on data from two conditions (e.g., an airplane in the upper visual field versus a carpet in the lower visual field), using a leave-one-out partitioning scheme (Figure 2B). The testing set consisted of all but one trials for each of the two conditions, while one trial for each of the two conditions was held back and used for classifier testing. This procedure was repeated until every trial was left out once. Classifier performance was averaged across these repetitions. The pairwise decoding analysis resulted in 12-by-12 matrix of decoding accuracies at each time point (reflecting all comparisons between the six objects appearing in the two locations) (Figure 2C).

2.6 Overall classification dynamics

To assess the overall classification dynamics over time, we computed the general discriminability of the twelve different conditions. All pairwise classification accuracies were averaged, revealing a time course of object decoding independently of the positional regularities. This time course of overall classification accuracy was used to define time points of interest at the peaks of the classification time series, where classification performance was particularly pronounced. Using a "region of interest" logic frequently applied in fMRI analyses (Poldrack, 2007), we used these peaks as "time points of interest" to increase the detection power of subsequent analyses.

2.7 Object classification in typical and atypical locations

To determine an effect of positional regularity on object decoding, we compared performance when classifying among typically positioned objects versus among atypically positioned objects. Pairwise classification accuracies were averaged for all comparisons between typically positioned objects (e.g., an airplane in the upper visual field versus a shoe in the lower visual field) and for all comparisons between atypically positioned

objects (e.g., a shoe in the upper visual field versus an airplane in the lower visual field) (Figure 2C). Subsequently, the two resulting classification time series (for typically and atypically positioned objects) were compared. To increase the statistical power of this comparison, we specifically focused on the effect of positional regularity at the peaks in overall classification.

2.8 *Sensor-space searchlight analysis*

To investigate which sensors contributed most to the observed effects, we performed a sensor-space searchlight analysis. For this analysis, the pairwise classification procedure was repeated for neighborhoods of seven adjacent electrodes around each individual electrode; the resulting classification accuracy was then mapped onto a scalp representation. This procedure allowed us to infer the approximate spatial distribution of classification differences between typically and atypically positioned objects. As for one participant only data from 32 electrodes was available, this participant was not included in the searchlight analysis.

2.9 *Statistical testing*

To identify significant effects across time we used a threshold-free cluster-enhancement procedure (Smith & Nichols, 2009) with default parameters. Multiple comparison correction was based on a sign-permutation test (with null distributions created from 10,000 bootstrapping iterations) as implemented in CoSMoMVPA (Oosterhof et al., 2016). The resulting statistical maps were thresholded at $Z > 1.96$ (i.e., $p < .05$). The same procedure was employed for identifying significant sites across electrodes in the sensor-space searchlight analysis. For assessing the significance of effects at the overall classification peaks, repeated-measures ANOVAs and paired *t*-tests were performed.

3 Results

3.1 Temporal dynamics of pairwise object classification

In a first step, we characterized the overall response dynamics observed in the pairwise classification analysis, which allowed us to restrict subsequent analyses to time points where classification performance was particularly pronounced. For this, we computed an overall measure of pairwise classification by averaging across all unique off-diagonal elements of the pairwise classification matrices (Figure 2C), resulting in a single classification time series. This analysis revealed robust above-chance classification starting from 70 ms after stimulus onset and prominently peaking at 140 ms and 220 ms (Figure 3A). These two clear peaks in the classification time series were used as time points of interest for subsequent analyses, as we reasoned that differences between typically and atypically positioned objects would be most pronounced at time points at which objects were most discriminable.

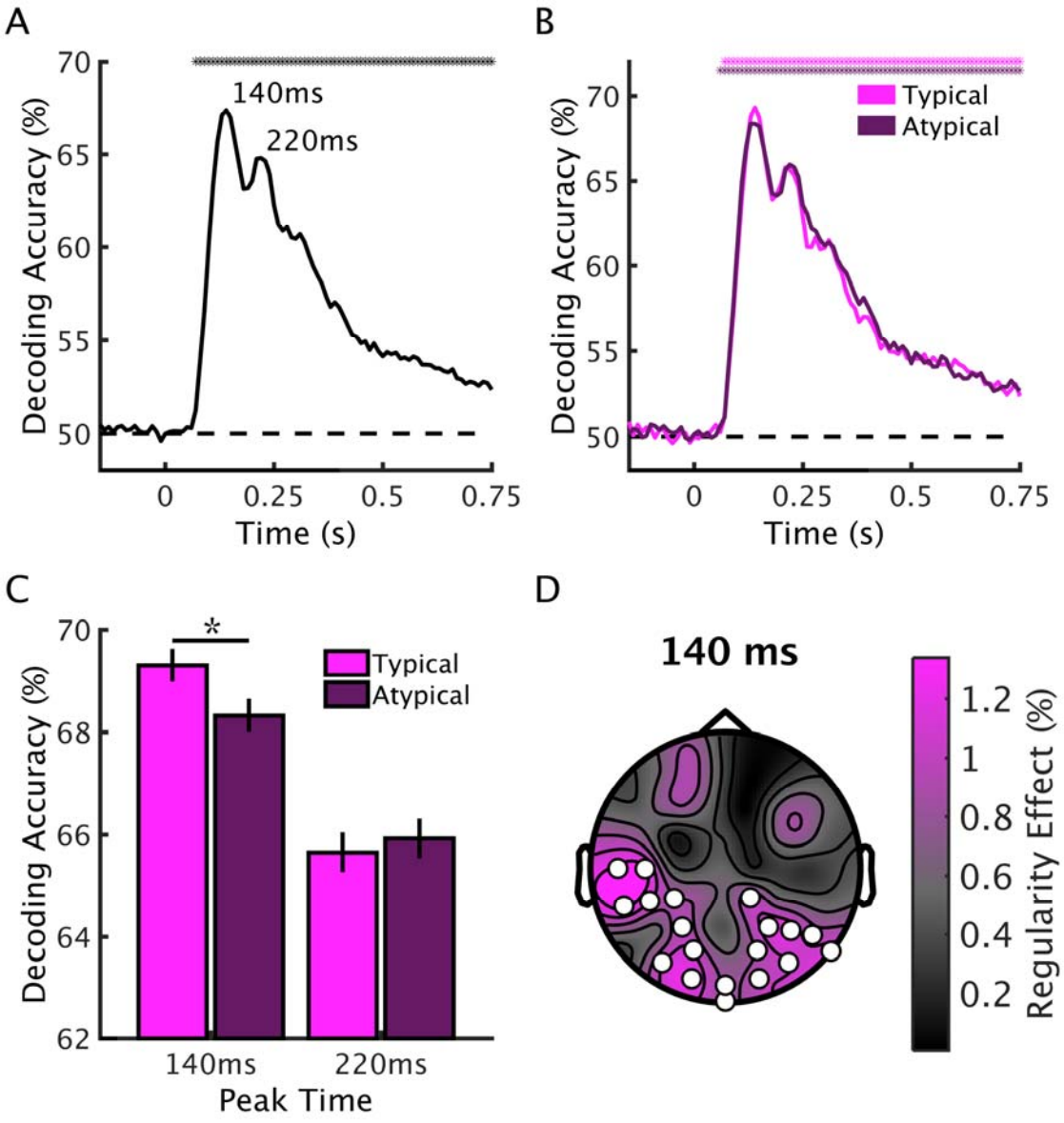

Figure 3. Classification Results. A) Overall pairwise classification performance was computed by averaging all pairwise decoding time series, revealing significant decoding accuracy starting at 70 ms after stimulus onset and peaking at 140 ms and 220 ms. Asterisks above data curves indicate above-chance classification ($p < .05$, corrected for multiple comparisons). B) Classification time series for typically and atypically positioned objects were computed by averaging all pairwise classification time series comparing typically and atypically positioned objects, respectively. Classification of typically and atypically positioned pairs showed comparable temporal dynamics, both peaking at the

time points identified in the overall decoding. Asterisks indicate above-chance classification ($p < .05$, corrected for multiple comparisons). C) At the first decoding peak (140 ms), but not the second peak (220 ms), classification was more accurate for typically than for atypically positioned objects. The asterisk indicates a significant difference ($p < .05$). Error bars reflect standard errors. D) A sensor-space classification searchlight revealed that the regularity effect (difference between the classification of typically and atypically positioned objects) at the 140 ms peak is most pronounced in occipital and temporal electrodes. Circles indicate electrodes exhibiting a significant regularity effect ($p < .05$, corrected for multiple comparisons).

3.2 Classification of objects when positioned typically and atypically

To test whether neural representations differ for typically and atypically positioned objects, we compared classification performance for all typically and all atypically positioned objects. We averaged all pairwise classification time courses that corresponded to comparisons within regular pairs (e.g., an airplane in the upper visual field versus a boat in the lower visual field) and comparisons within irregular pairs (e.g., an airplane in the lower visual field versus a boat in the upper visual field) (Figure 3B). The classification time series for typically and atypically positioned objects showed a similar temporal structure and both replicated the peak structure observed in the overall decoding, allowing for a meaningful comparison between typically and atypically positioned objects at the classification peaks. We thus restricted statistical comparisons to two time points of interest: the peak times observed in the overall decoding (140 ms and 220 ms). For the early peak at 140ms, we found higher classification accuracy for typically than for atypically positioned objects, $t(33) = 3.04$, $p = .005$, while for the later

peak at 220ms, no such difference emerged, $t(33) = 0.69$, $p = .495$, interaction with peak time, $F(1,33) = 7.44$, $p = .010$ (Figure 3C). This pattern of results suggests that earlier stages of object processing (as reflected in the decoding peak at 140 ms) benefit from typical object locations, while relatively later object representations (at 220 ms after stimulus onset) are not sensitive to positional regularities.

To estimate the spatial extent of the early regularity effect, we performed a searchlight analysis in sensor space. We repeatedly performed the pairwise classification analysis for neighborhoods of seven adjacent sensors, using only data from the early peak at 140 ms. To quantify the regularity benefit, we then computed the difference between all pairwise comparisons of typically positioned objects and all pairwise comparisons of atypically positioned objects at every sensor location. This analysis revealed a significant regularity effect in posterior and lateral electrodes (19 significant electrode sites) (Figure 3D), suggesting that the enhanced classification for regularly positioned objects originates from visual areas of the occipital and temporal cortices.

3.3 Classification within and between locations

Our classification approach collapsed across pairwise comparisons within the same location and between different locations, so that classifiers could rely on information from both an object's identity and its location. A recent study on location priors in face-part processing (de Haas et al., 2016) has found effects of positional regularities only when comparing response patterns between locations. To investigate whether also the regularity effects for objects are differently pronounced when classifying between the two locations or within the same location, we separately looked at the regularity effect for all comparisons between locations (e.g., an airplane in the upper visual field versus a shoe in the lower visual field) (Figure 4A) and all comparisons

within location (e.g., an airplane in the upper visual field versus a hat in the upper visual field) (Figure 4B). We found a main effect of visual field comparison, $F(1,33) = 365.70$, $p < .001$, with higher classification accuracies for classifying between locations (where the classifier can use the stimulus' location) than within location (where the classifier has no location information available), and an interaction of the within-between comparison and peak latency, $F(1,33) = 72.30$, $p < .001$, with a relatively more pronounced early peak when classifying between locations. Replicating our previous results, the analysis produced a significant peak X regularity interaction, $F(1,33) = 9.83$, $p = .004$, with a regularity benefit at the 140 ms peak, $t(33) = 3.15$, $p = .004$, but not the 220 ms peak, $t(33) = 1.05$, $p = .301$. Crucially, this pattern of results did not depend on the type of classification (between locations versus within location), $F(1,33) = 2.53$, $p = .121$, suggesting that typical real-world locations comparably boost early object classification when objects appear in similar or different locations (Figure 4C,D).

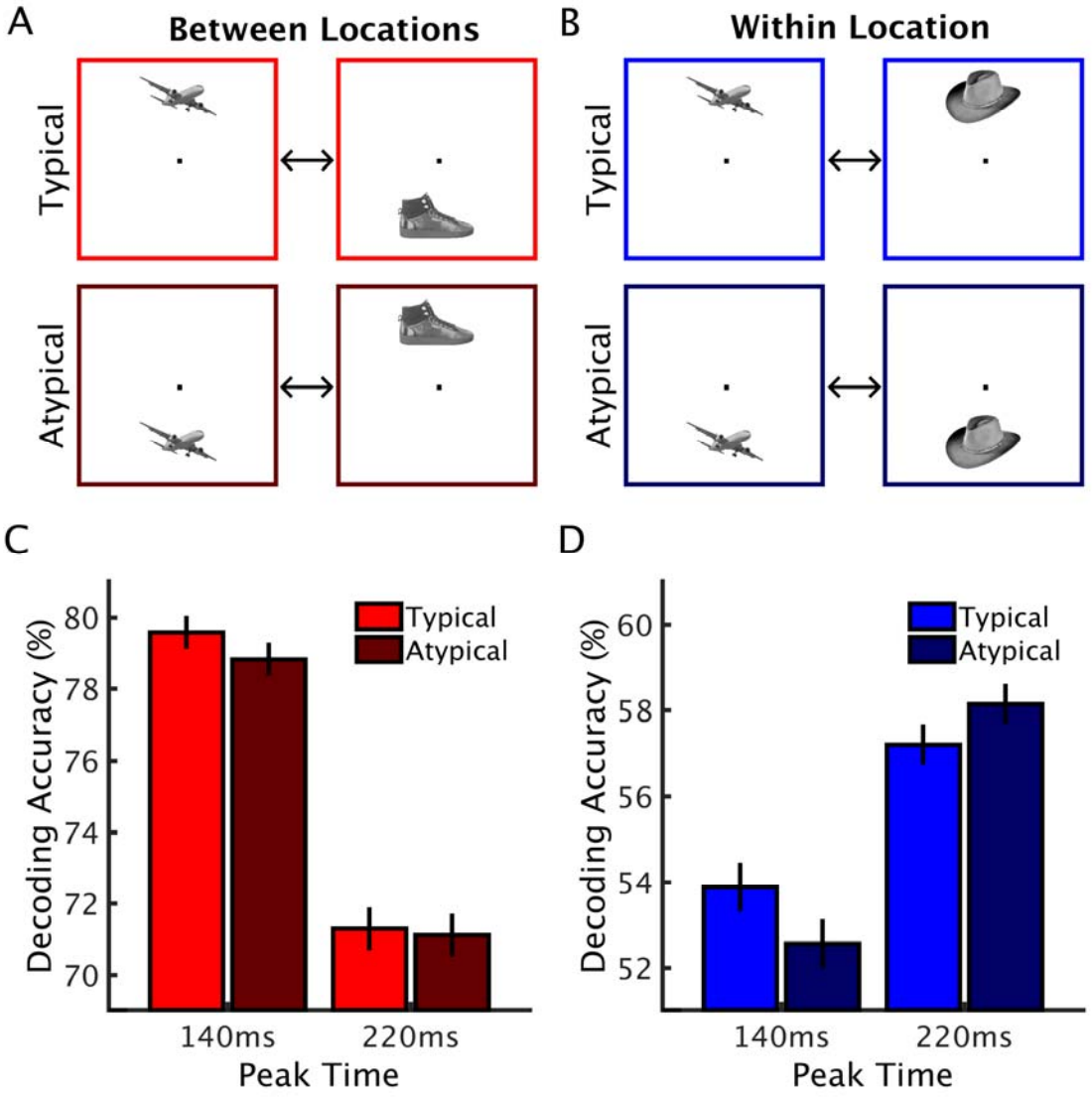

Figure 4. Between-Locations versus Within-Location Classification. We compared peak decoding for typically and atypically positioned objects separately for comparisons between different locations (e.g., an airplane in the upper visual field versus a shoe in the lower visual field) (A) and within the same location (e.g., an airplane in the upper visual field versus a hat in the upper visual field) (B). For both comparison types, we found a similar pattern (C, D) with a benefit for typically positioned objects at the 140 ms peak. Importantly, the patterns of results for between-locations and within-location classification were statistically indistinguishable (see Results). Error bars reflect standard errors.

4 Discussion

4.1 Summary

Here, we demonstrate that positional regularities contained in real-world scenes impact brain responses to individual objects. Using multivariate classification of EEG data, we show that object coding across the visual field is affected by the typical real-world location of the object. When objects are presented in frequently experienced locations, EEG response patterns at 140 ms after stimulus onset are better discriminable than when the same objects are presented in atypical locations. This advantage for typically positioned objects was equally pronounced for classification between locations and within the same location. Using a sensor-space searchlight analysis, we show that the effect was primarily localized in posterior and lateral sensors, suggesting that typically positioned objects gain an advantage during early perceptual processing.

4.2 Early stages of object coding are sensitive to typical locations

Our results support the hypothesis that extensive experience with natural scene structure can enhance object coding when objects appear in typical locations of the visual field. This finding demonstrates that visual processing channels are preferentially tuned to specific objects appearing in specific locations (Kaiser & Haselhuhn, 2017; Kravitz et al., 2008). Crucially, our EEG classification approach allowed us to pinpoint the latency of this regularity benefit: We demonstrate that object processing at 140 ms after stimulus onset is affected by positional regularity. The timing of the effect suggests that objects appearing in typical visual field locations gain an advantage during early, perceptual processing, rather than through top-down interactions within visual cortex or feedback from frontal areas; previous M/EEG studies have suggested that such feedback processes impact visual responses only at later stages, starting shortly before 200 ms (Bar et al.,

2006; Fahrenfort, van Leeuwen, Olivers, & Hogendoorn, 2017). As opposed to the difference in early object processing, later representations (at 220 ms after stimulus onset) do not depend on the location of the object. This result concurs with the increasing location tolerance over the time course of object classification, peaking at around 180 ms (Isik et al., 2014), mirroring the increase in receptive field size along the visual stream (Kravitz, Saleem, Baker, Ungerleider, & Mishkin, 2013).

4.3 Visual versus categorical sources of the regularity benefit

What is the content of the location-specific object representations emerging at 140 ms? Peaks in the M/EEG decoding in this time range have been previously associated with visual category processing in object-selective cortex (Cichy, Pantazis, & Oliva, 2014, 2016; Carlson et al., 2013). Our searchlight analysis reveals the strongest regularity effect over lateral occipital and temporal electrode sites, suggesting that the effect originates from object-selective visual cortex. Whether processing differences in these object-selective regions reflect genuine category processing differences or whether they reflect differential coding of category-associated visual features is a debated question (Bracci, Ritchie, & op de Beeck, 2017; Peelen & Downing, 2017). While some data suggest that visual properties explain most of the variance in object-selective responses (e.g., Baldassi et al., 2013), a recent MEG decoding study has demonstrated category-selective, rather than visually (shape-) driven, responses from as early as 130 ms after stimulus onset (Kaiser, Azzalini, & Peelen, 2016). To determine if the regularity benefit observed here can be linked to differences in the processing of particular visual features or true categorical processing differences, future studies need to employ stimuli that vary more extensively in their visual characteristics.

4.4 Positional structures in multiple and individual objects

Natural environments contain positional regularities on different levels, both on the levels of multiple (e.g., a lamps typically hang above tables) and individual objects (e.g., a lamp is typically in the upper visual field). Previous research has primarily focused on the latter: Recent behavioral studies have demonstrated that regularity structures in multi-object arrangement facilitate behavior in capacity-limited visual tasks (Gronau & Shachar, 2014; Kaiser et al., 2014; Kaiser, Stein, & Peelen, 2015; Stein, Kaiser, & Peelen, 2015), and neuroimaging studies demonstrated that they enable the brain to integrate information across objects that appear in frequently experienced arrangements (Baeck, Wagemans, & Op de Beeck, 2013; Kaiser & Peelen, 2017; Kaiser et al., 2014).

Here, we provide the first evidence that typical regularity structures also impact the neural representation of individual objects. Our finding thus raises the question whether the previously reported regularity effects in multi-object perception can be reduced to the effects of typical individual object location. On a behavioral level, some previous studies oppose this notion by demonstrating that the benefits of multi-object regularities cannot be explained by the relative location of the constituent objects (Kaiser et al., 2014, 2015; Stein et al., 2015). Although these results suggest that positional regularities in multi-object and single-object processing offer complementary benefits, further research is needed. Future studies will need to systematically manipulate positional structures on different levels (from individual objects to multi-object arrangements) to explore how regularities on multiple levels interact on a neural level.

4.5 Positional structures beyond person perception

Positional regularities have been studied in humans and non-human primates largely in the context of face and body perception, where parts are arranged in highly predictable configurations (e.g., the features of a human face). fMRI studies in humans

have demonstrated that individual face and body parts are processed more efficiently when they appear in typical visual field locations (Chan et al., 2010; de Haas et al., 2016). Single-cell recordings in monkeys demonstrated that location biases can impact cortical responses to face parts as early as 100 ms after stimulus onset (Issa & DiCarlo, 2012), suggesting a benefit at early stages of perceptual processing.

Our results complement these findings by showing that such location-specific object processing is not restricted to the face/body domain: The inherent structure of natural scenes can similarly impact early processing (140 ms after stimulus onset) of object information across the visual field. Our findings thus highlight that location-specific tuning in object processing may form a general principle that shapes visual processing mechanisms for spatially predictable information. Future research could test whether regularity structures also affect other domains where the visual input consists of multiple parts that are constrained by spatial regularities. For example, through extensive experience with reading written text, the neural mechanisms for perceiving letters could get tuned to their typical spatial locations within words (Kaiser & Haselhuhn, 2017; Vinckier et al., 2007).

4.6 Location-specific object coding and efficient scene perception

A major challenge for the visual system when processing natural scenes is the large number of individual objects they contain. The concurrent representation of multiple objects is limited by an overlap in processing resources, as indexed by reduced neural responses when multiple objects need to be processed (Cohen, Konkle, Rhee, Nakayama, & Alvarez, 2014; Desimone & Duncan, 1995; Franconeri, Alvarez, & Cavanagh, 2013). The preferential coding for typically positioned objects revealed here may contribute to efficient scene processing by reducing this inter-object competition. By

457 coding the objects of a scene via separable location-specific processing channels that are
458 optimally tuned to objects typically appearing in these locations, the overlap in neural
459 processing resources can be reduced. Linking this increase in neural efficiency to a
460 facilitation of perceptual performance could help to understand the efficient processing
461 of highly complex natural environments.

Acknowledgements

The research was supported by a DFG Emmy-Noether Grant awarded to R.M.C. (Cl241-1/1).

References

Baeck, A., Wagemans, J., & Op de Beeck, H. P. (2013). The distributed representation of random and meaningful object pairs in human occipitotemporal cortex: the weighted average as a general rule. *Neuroimage, 70,* 37-47.

Baldassi, C., Alemi-Neissi, A., Pagan, M., DiCarlo, J. J., Zecchina, R., & Zoccolan, D. (2013). Shape similarity, better than semantic membership, accounts for the structure of visual object representations in a population of monkey inferotemporal neurons. *PLoS Computational Biology, 9,* e1003167.

Bar, M. (2004). Visual objects in context. *Nature Reviews Neuroscience, 5,* 617-629.

Bar, M., Kassam, K. S., Ghuman, A. S., Boshyan, J., Schmid, A. M., Dale, A. M., Hämäläinen, M. S., Marinkovic, K., Schacter, D. L., Rosen, B. R., & Halgren, E. (2006). Top-down facilitation of visual recognition. *Proceedings of the National Academy of Sciences, U.S.A., 103,* 449-454.

Biederman, I., Mezzanotte, R. J., & Rabinowitz, J. C. (1982). Scene perception: detecting and judging objects undergoing relational violations. *Cognitive Psychology, 14,* 143-177.

Bracci, S., Ritchie, J. B., & op de Beeck, H. P. (2017). On the partnership between neural representations of object categories and visual features in the ventral visual pathway. *Neuropsychologia,* doi:10.1016/j.neuropsychologia.2017.06.010.

Brainard, D. H. (1997). The psychophysics toolbox. *Spatial Vision, 10,* 433-436.

Carlson, T. A., Hogendoorn, H., Kanai, R., Mesik, J., & Turret, J. (2011). High temporal resolution decoding of object position and category. *Journal of Vision, 11,* 9.

Carlson, T. A., Tovar D. A., Alink, A., & Kriegeskorte, N. (2013). Representational dynamics of object vision: the first 1000 ms. *Journal of Vision, 13,* 1-19.

488 Chan, A. W., Kravitz, D. J., Truong, S., Arizpe, J., & Baker, C.I. (2010). Cortical
489 representations of bodies and faces are strongest in commonly experienced
490 configurations. *Nature Neuroscience, 13,* 417-418.
491 Chun, M. M. (2000). Contextual cueing of visual attention. *Trends in Cognitive Sciences, 4,*
492 170-178.
493 Cichy, R. M., Chen, Y., & Haynes, J. D. (2011). Encoding the identity and location of objects
494 in human LOC. *Neuroimage, 54,* 2297-2307.
495 Cichy, R. M., Pantazis, D., & Oliva, A. (2014). Resolving human object recognition in space
496 and time. *Nature Neuroscience, 17,* 455-462.
497 Cichy, R. M., Pantazis, D., & Oliva, A. (2016). Similarity-based fusion of MEG and fMRI
498 reveals spatio-temporal dynamics in human cortex during visual object
499 recognition. *Cerebral Cortex, 26,* 3563-3579.
500 Cohen, M. A., Konkle, T., Rhee, J. Y., Nakayama, K., & Alvarez, G. A. (2014). Processing of
501 multiple visual objects is limited by overlap in neural channels. *Proceedings of the*
502 *National Academy of Sciences, U.S.A., 111,* 8955-8960.
503 Contini, E. W., Wardle, S. G., & Carlson, T. A. (2017). Decoding the time-course of object
504 recognition in the human brain: From visual features to categorical decisions.
505 *Neuropsychologia,* doi:10.1016/j.neuropsychologia.2017.02.013.
506 de Haas, B., Schwarzkopf, D. S., Alvarez, I., Lawson, R. P., Henriksson, L., Kriegeskorte, N.,
507 & Rees, G. (2016). Perception and processing of faces in the human brain is tuned
508 to typical facial feature locations. *Journal of Neuroscience, 36,* 9289-9302.
509 Desimone, R., & Duncan, J. (1995). Neural mechanisms of selective visual attention.
510 *Annual Review of Neuroscience, 18,* 193-222.

511 Fahrenfort, J. J., van Leeuwen, J., Olivers, C. N. L., & Hogendoorn, H. (2017). Perceptual
512 integration without conscious access. *Proceedings of the National Academy of*
513 *Sciences, U.S.A., 114,* 3744-3749.
514 Franconeri, S. L., Alvarez, G. A., & Cavanagh, P. (2013). Flexible cognitive resources:
515 competitive content maps for attention and memory. *Trends in Cognitive Sciences,*
516 *17,* 134-141.
517 Golomb, J. D., & Kanwisher, N. (2012). Higher level visual cortex represents retinotopic,
518 not spatiotopic, object location. *Cerebral Cortex, 22,* 2794-2810.
519 Gronau, N., & Shachar, M. (2014). Contextual integration of visual objects necessitates
520 attention. *Attention, Perception & Psychophysics, 76,* 695-714.
521 Hasson, U., Levy, I., Behrmann, M., Hendler, T., & Malach, R. (2002). Eccentricity bias as an
522 organizing principle for human high-order object areas. Neuron, *34,* 479-490.
523 Hemond, C. C., Kanwisher, N., & Op de Beeck, H. P. (2007). A preference for contralateral
524 stimuli in human object- and face-selective cortex. *PLoS One,* 2, e574.
525 Henriksson, L., Mur, M., & Kriegeskorte, N. (2015). Faciotopy – A face-feature like
526 topology in the human occipital face area. *Cortex*, 72, 156-167.
527 Hong, H, Yamins, D. L. K., Majaj, N. J., & DiCarlo, J. J. (2016). Explicit information for
528 category-orthogonal object properties increases along the ventral visual stream.
529 *Nature Neuroscience, 19,* 613-622.
530 Isik, L., Meyers, E. M., Leibo, J. Z., & Poggio, T. (2014). The dynamics of invariant object
531 recognition in the human visual system. *Journal of Neurophysiology, 111,* 91-102.
532 Issa, E. B., & DiCarlo, J. J. (2012). Precedence of the eye region in neural processing of
533 faces. *Journal of Neuroscience, 32,* 16666-16682.

534 Kaiser, D., Azzalini, D. C., & Peelen, M. V. (2016). Shape-independent object category
535 responses revealed by MEG and fMRI decoding. *Journal of Neurophysiology, 115,*
536 2246-2250.
537 Kaiser, D., & Haselhuhn, T. (2017). Facing a regular world: How spatial object structure
538 shapes visual processing. *Journal of Neuroscience, 37,* 1965-1967.
539 Kaiser. D., & Peelen, M. V. (2017). Transformation from independent to integrative coding
540 of multi-object arrangements in human visual cortex. *BioRxiv*, doi:10.1101/117432.
541 Kaiser, D., Stein, T., & Peelen, M. V. (2014). Object grouping based on real-world
542 regularities facilitates perception by reducing competitive interactions in visual
543 cortex. *Proceedings of the National Academy of Sciences, U.S.A., 111,* 11217-11222.
544 Kaiser, D., Stein, T., & Peelen, M. V. (2015). Real-world spatial regularities affect visual
545 working memory for objects. *Psychonomic Bulletin & Review*, 22, 1784-1790.
546 Kravitz, D. J., Kriegeskorte, N., & Baker, C. I. (2010). High-level visual object
547 representations are constrained by position. *Cerebral Cortex, 20,* 2916-2925.
548 Kravitz, D. J., Saleem, K. S., Baker, C. I., Ungerleider, L. G., & Mishkin, M. (2013). The
549 ventral visual pathway: an expanded neural framework for the processing of
550 object quality. *Trends in Cognitive Sciences, 17,* 26-49.
551 Kravitz, D. J., Vinson, L. D., & Baker, C. I. (2008). How position dependent is visual object
552 recognition? *Trends in Cognitive Sciences, 12,* 114-122.
553 Oliva, A., & Torralba, A. (2007). The role of context in object recognition. *Trends in*
554 *Cognitive Sciences, 11,* 520-527.
555 Oostenveld, R., Fries, P., Maris, E., & Schoffelen, J. M. (2011). Fieldtrip: open source
556 software for advances analysis of MEG, EEG, and invasive electrophysiological
557 data. *Computational Intelligence and Neuroscience, 2011,* 156869.

558 Oosterhof, N. N., Connolly, A. C., & Haxby, J. V. (2016). CoSMoMVPA: multi-modal
559 multivariate pattern analysis of neuroimaging data in Matlab / GNU Octave.
560 *Frontiers in Neuroinformatics, 10*, 20.
561 Peelen, M. V., & Downing, P. E. (2017) Category selectivity in human visual cortex: Beyond
562 visual object recognition. *Neuropsychologia,*
563 doi:10.1016/j.neuropsychologia.2017.03.033.
564 Poldrack, R. A. (2007). Region of interest analysis for fMRI. *Social Cognitive and Affective*
565 *Neuroscience, 2*, 67-70.
566 Russell, B. C., Torralba, A., Murphy, K. P., & Freeman, W. T. (2008). LabelMe: a database
567 and web-based tool for image annotation. *International Journal of Computer Vision,*
568 *77*, 157-173.
569 Schwarzlose, R. F., Swisher, J. D., Dang, S., & Kanwisher, N. (2008). The distribution of
570 category and location information across object-selective regions in human visual
571 cortex. *Proceedings of the National Academy of Sciences, U.S.A., 105*, 4447-4452.
572 Smith, S. M., & Nichols, T. E. (2009). Threshold-free cluster enhancement: addressing
573 problems of smoothing, threshold dependence and localization in cluster
574 interference. *Neuroimage, 66, 215*-222.
575 Stein, T., Kaiser, D., & Peelen, M. V. (2015). Interobject grouping facilitates visual
576 awareness. *Journal of Vision, 15*, 10.
577 Vinckier, F., Dehaene, S., Jobert, A., Dubus, J. P., Sigman, M., & Cohen, L. (2007).
578 Hierarchical coding of letter strings in the ventral stream: dissecting the inner
579 organization of the visual word-form system. *Neuron, 55*, 143-156.

Willenbockel, V., Sadr, J., Fiset, D., Horne, G. O., Gosselin, F., & Tanaka, J. W. (2010). Controlling low-level image properties: The SHINE toolbox. *Behavior Research Methods, 42,* 671-684.

Wolfe, J. M., Võ, M. L.-H., Evans, K. K., & Greene, M. R. (2011). Visual search in scenes involves selective and nonselective pathways. *Trends in Cognitive Sciences, 15,* 77-84.